



Spinal cord and brain tissue impairments as long-term effects of rugby practice? An exploratory study based on T1 and ihMTsat measures

Arash Forodighasemabadi, Guillaume Baucher, Lucas Soustelle, Thomas Troalen, Olivier Girard, Maxime Guye, Jean-Baptiste Grisoli, Jean-Philippe Ranjeva, Guillaume Duhamel, Virginie Callot

► To cite this version:

Arash Forodighasemabadi, Guillaume Baucher, Lucas Soustelle, Thomas Troalen, Olivier Girard, et al.. Spinal cord and brain tissue impairments as long-term effects of rugby practice? An exploratory study based on T1 and ihMTsat measures. *Neuroimage-Clinical*, 2022, 35, pp.103124. 10.1016/j.nicl.2022.103124 . hal-03770501

HAL Id: hal-03770501

<https://amu.hal.science/hal-03770501>

Submitted on 6 Sep 2022

HAL is a multi-disciplinary open access archive for the deposit and dissemination of scientific research documents, whether they are published or not. The documents may come from teaching and research institutions in France or abroad, or from public or private research centers.

L'archive ouverte pluridisciplinaire **HAL**, est destinée au dépôt et à la diffusion de documents scientifiques de niveau recherche, publiés ou non, émanant des établissements d'enseignement et de recherche français ou étrangers, des laboratoires publics ou privés.



Distributed under a Creative Commons Attribution - NonCommercial - NoDerivatives 4.0 International License

Spinal cord and brain tissue impairments as long-term effects of rugby practice? An exploratory study based on T₁ and ihMTsat measures.

Authors

Arash Forodighasemabadi^{1,2,3,4}, Guillaume Baucher^{1,2,5}, Lucas Soustelle^{1,2}, Thomas Troalen⁶, Olivier M. Girard^{1,2}, Maxime Guye^{1,2}, Jean-Baptiste Grisoli⁷, Jean-Philippe Ranjeva^{1,2}, Guillaume Duhamel^{1,2}, and Virginie Callot^{1,2,4,*}

Affiliations

1 Aix-Marseille Univ, CNRS, CRMBM, Marseille, France

2 APMH, Hopital Universitaire Timone, CEMEREM, Marseille, France

3 Aix-Marseille Univ, Université Gustave Eiffel, LBA, Marseille, France

4 iLab-Spine International Associated Laboratory, Marseille-Montreal, France-Canada

5 APMH, Hopital Universitaire Nord, Neurosurgery Dept, Marseille, France

6 Siemens Healthcare SAS, Saint-Denis, France

7 APMH, Hopital Universitaire Timone, Pôle MPR, Marseille, France

*** Corresponding author**

Virginie Callot

CRMBM-CEMEREM, UMR 7339, CNRS - Aix-Marseille Université, Faculté de Médecine

27, bd Jean Moulin, 13385 Marseille Cedex 5, France.

virginie.callot@univ-amu.fr

Tel: +33491388465

CRedit roles

Arash Forodighasemabadi: Conceptualization; Data curation; Formal analysis; Investigation; Methodology; Software; Validation; Visualization; Roles/Writing - original draft; Writing - review & editing

Guillaume Baucher: Formal analysis; Investigation; Methodology; Visualization; Writing - review & editing

34 Lucas Soustelle: Formal analysis; Methodology; Software; Writing - review & editing
35
36 Thomas Troalen: Methodology; Writing - review & editing
37
38 Olivier M. Girard: Conceptualization; Formal analysis; Methodology; Validation; Writing -
39 review & editing
40
41 Maxime Guye: Project administration; Resources.
42
43 Jean-Baptiste Grisoli : Conceptualization ; Data curation ; Resources
44
45 Jean-Philippe Ranjeva: Conceptualization; Formal analysis; Validation; Writing - review &
46 editing
47
48 Guillaume Duhamel: Conceptualization; Formal analysis; Methodology; Validation ; Writing
49 - review & editing
50
51 Virginie Callot: Conceptualization; Data curation ; Formal analysis ; Funding acquisition;
52 Investigation ; Methodology ; Project administration ; Resources ; Supervision ; Validation ;
53 Visualization ; Writing - review & editing
54
55
56
57
58
59
60
61
62
63 **Abbreviations**
64 CSA: Cross-Sectional Area
65 cSC: Cervical Spinal Cord
66 CSF: Cerebrospinal Fluid
67 CST: Corticospinal Tracts

68 GM: Gray Matter
69 HC: Healthy Control
70 ihMT: inhomogeneous Magnetization Transfer
71 LST: Lateral Sensory Tracts
72 mJOA: Modified Japanese Orthopedic Association
73 MP2RAGE: Magnetization Prepared 2 Rapid Acquisition Gradient Echo
74 NDI: Neck Disability Index
75 OSS: Overall Stenosis Score
76 PST: Posterior Sensory Tracts
77 R: Rugby player
78 RST: Reticulo/Rubrospinal Tracts
79 WM: White Matter

80
81

82 **Highlights**

83
84

- 85 • Diffuse degeneration of spinal cord (higher T_1) is observed in retired rugby players
- 86
- 87 • Demyelination of brain WM tracts (higher T_1 / lower ihMTsat values) is present in
- 88 rugby players
- 89
- 90 • Early aging in both brain and spinal cord tissues may be linked to the rugby practice
- 91
- 92 • The aforementioned effects may suggest cumulative effects of long-term impacts on
- 93 the tissues
- 94
- 95

Abstract

Rugby players are subject to multiple impacts to their head and neck that could have adverse neurological effects and put them at increased risk of neurodegeneration.

Previous studies demonstrated altered default mode network and diffusion metrics on brain, as well as more foraminal stenosis, disc protrusion and neck pain among players of contact sports as compared to healthy controls. However, the long-term effects of practice and repetitive impacts on brain and cervical spinal cord (cSC) of the rugby players has never been systematically investigated.

In this study, 15 retired professional and amateur rugby players (R) and 15 age-matched healthy controls (HC) (all males; mean age R: 46.8 ± 7.6 ; and HC: 48.6 ± 9.5) were recruited both to investigate cord impairments and further characterize brain structure damage. Medical questionnaires including modified Japanese Orthopedic Association scale (mJOA) and Neck Disability Index (NDI) were filled by all participants. A 3T multi-parametric MR protocol including conventional qualitative techniques such as T_1 -, T_2 -, and T_2^* -weighted sequences, as well as state-of-the art quantitative techniques including MP2RAGE T_1 mapping and 3D ihMT-RAGE, was used on both brain and cSC. Normalized brain WM and GM volumes, spine Overall Stenosis Score, cord cross-sectional area and regional T_1 and ihMT metrics were derived from these acquisitions.

Rugby players showed significantly higher NDI scores, as well as a faster decline of normalized brain GM volume with age as compared to HC. Moreover, higher T_1 values on cSC suggestive of structural degeneration, together with higher T_1 and lower ihMTsat on brain WM suggestive of demyelination, were observed in retired rugby players as compared to age-matched controls, which may suggest cumulative effects of long-term impacts on the tissues. Metrics also suggest early aging and different aging processes on brain tissue in the players.

These preliminary observations provide new insights in the domain, which should now be further investigated on larger cohorts and multicentric longitudinal studies, and further correlated to the likelihood of neurodegenerative diseases and risk factors.

Keywords

Rugby, Brain, Cervical spinal cord, T_1 MP2RAGE, inhomogeneous Magnetization Transfer, Neurodegeneration.

1 Introduction

Players of contact sports, such as rugby, receive repetitive impacts to their head and neck that do not necessarily result in observable injuries¹. However, there have been several studies demonstrating the adverse effects of these impacts on the health of players. Most of these studies, focusing on the brain, demonstrated that rugby players, even without a history of concussion, may present lower visuomotor processing speed², more cognitive vulnerability³ and longer reaction times⁴ compared to age-matched controls. Diffusion Tensor Imaging (DTI) and functional MRI (fMRI) studies on brain have also demonstrated impaired microstructure with decreased Fractional Anisotropy (FA) in multiple white matter (WM) tracts accompanied with default mode network and visual network hyperconnectivity in rugby players in-season as compared to off-season, which was not observed in players of non-contact sports⁵. On spine, rugby players were found to have more chronic neck pain and foraminal stenosis, narrower vertebral canal, and more substantial osteophytes as compared to age-matched healthy controls^{6,7}. However, no studies have been conducted so far to characterize potential effects on the cervical spinal cord (cSC) itself.

In this study, we propose to use complementary state-of-the-art quantitative MRI techniques that have been recently adapted to brain and SC imaging at 3 T to scan retired rugby players that have played in amateur and professional leagues. The protocol included a fast 3D Magnetization Prepared 2 Rapid Acquisition Gradient Echo (MP2RAGE) T₁ mapping of both brain and cervical cord⁸, as well as the recent 3D inhomogeneous Magnetization Transfer with rapid acquisition gradient echo technique (ihMTRAGE)⁹. Conventional T₁ relaxometry has already been used widely to study tissue alterations in pathologies such as Multiple Sclerosis (MS) or Parkinson's disease (PD)¹⁰⁻¹², where it was demonstrated to be sensitive to demyelination, iron deposition or structural variations. Interestingly demyelination and iron accumulation could affect T₁ in opposite directions¹³, T₁ could therefore lack specificity if both phenomena are present. The ihMT method, on the other hand, is more specific to myelin in central nervous system (CNS) tissues¹⁴⁻¹⁷. It has been used in several clinical and preclinical studies on brain^{14,16,18-23} and recently adapted to SC imaging to study demyelinating pathologies such as MS and normal aging²⁴⁻²⁷.

By comparing brain and cSC T₁ and ihMT metrics collected on both retired players and age-matched healthy controls, this work investigated whether the cord is impaired and early tissue

aging occurs in the rugby player population, while refining previously reported brain tissue structure damage description.

2 Materials & Methods

2.1 Subjects and clinical assessments

Fifteen retired rugby players (all males; 7 professionals and 8 amateurs) without known neurodegenerative disease and with no prior cervical spine surgery were enrolled in the study, together with 15 aged- and sex-matched healthy controls. Demographic data are summarized in Table 2. The local ethics committee of our institution approved the protocol and written informed consent was obtained from each participant.

Modified Japanese Orthopedic Association score (mJOA)²⁸ and neck pain (Neck Disability Index (NDI))²⁹ questionnaires were filled by the participants to evaluate motor and sensory dysfunction.

2.2 MR protocol

The subjects were scanned with a multi-parametric MR protocol using a 3T MR system (MAGNETOM Vida, Siemens Healthcare, Erlangen, Germany) with a 20-channel head and neck coil. Neck and brachial plexus MRI pads (Sat Pad Clinical Imaging Solutions, West Chester, PA, USA) were installed around the subject neck and shoulders to reduce the B_0 magnetic field inhomogeneity. When possible for the subject, the RF coil was tilted to place the cord as straight as possible and hence minimize partial volume effects (PVE) encountered with non-isotropic sequences due to the cord curvature.

The multi-parametric MRI protocol included conventional anatomical techniques, as well as quantitative MP2RAGE⁸ and ihMTRAGE⁹ sequences, as detailed in Table 1. T_2^* and ihMT slices were placed perpendicular to the cord to minimize PVE. The MP2RAGE and ihMT techniques are detailed in the following sections. The protocol also included a B_1^+ map acquired using a pre-saturated turbo flash (TFL) sequence³⁰ to correct quantitative T_1 values and ihMT signal from B_1^+ inhomogeneities (see below). The whole protocol lasted 50 minutes.

Sequence	Region	Orientation	Resolution (mm ³)	TR (s)	FOV (mm ²)	Acq. Time (min)	Information / MR metrics of interest
T₂w TSE	SC	SAG	0.6×0.6×3	3500	220×220	1:47	Disc protrusion
T₂w	SC	SAG	0.6×0.6×1	1500	256×256	2:42	Antero-posterior and right-

SPACE							left diameter of cord and canal; Foraminal stenosis
T ₂ *w MGE	SC	TRA	0.4×0.4×5	1400	180×180	5:04	GM, WM, and SC CSA
T ₂ w FLAIR	Brain	TRA	0.9×0.9×5	10000	240×180	2:42	Investigating (lack of) major brain abnormalities
Presat TFL	SC+Brain	SAG	5×5×5	5000	320×320	10 s	B ₁ ⁺ map used to correct T ₁ and ihMT-bias
ihMT RAGE	SC	TRA	0.9×0.9×10	2500	180×180	9:47	ihMTsat maps
	Brain		2×2×2		256×200	13:34	
	Specific parameters						
	Low Duty Cycle (DC) high RF power ihMT preparation: train of ten 5ms-pulses (Tukey-shaped pulses with a cosine fraction of r=0.2 ³¹ ; B ₁ -peak=14.13 μT; Cosine-modulated pulses for the dual-offset saturation ^{9,21} ; repeated every 100ms (DC=5%); total saturation time 1s; B ₁ -RMS=2.95 μT; frequency offset (f) 7 kHz. Five volumes on brain: M0, MT+, MT±, MT-, MT± and 13 volumes on SC: M0+3 repetitions of (MT+, MT±, MT-, MT±).						
MP2RAGE	Brain+SC (single acquisition)	SAG	0.9×0.9×0.9	6.2	315×258	8:02	T ₁ quantitative maps; Normalized GM/WM volume
	Specific parameters						
T11/TI2/α ₁ /α ₂ =650 ms/3150 ms/5°/3°; GRAPPA=2; Partial Fourier=6/8 ; MP2RAGE TR 4000 ms							

Table 1: Multi-parametric MR protocol used for the study and derived metrics. TSE: Turbo Spin Echo; SPACE: Sampling Perfection with Application-optimized Contrasts using different flip angle Evolution (Siemens); MGE: Multi Gradient Echo; FLAIR: FLuid-Attenuated Inversion Recovery; CSA: Cross-Sectional Area; GM: Gray Matter; WM: White Matter.

2.2.1 Magnetization Prepared 2 Rapid Acquisition Gradient Echo

MP2RAGE is an Inversion Recovery (IR)-based technique that acquires two RAGE volumes in an interleaved manner, from which a uniform (UNI) image is derived, which can then be used to estimate the T₁ of the tissue voxel-wise. Originally proposed for the brain³² and widely used to study pathologies like MS^{33–36}, this technique was then optimized to study healthy and pathological cervical cord^{37–40}. Recently tuned at 3T with regards to CNR and B₁⁺ insensitivity to study both brain and cSC simultaneously⁸, this latter setup was used in the present study. Potential T₁ imperfections due to residual B₁⁺ inhomogeneities were corrected using a B₁⁺ map as in³⁷.

2.2.2 Inhomogeneous Magnetization Transfer

IhMT has recently been proposed and validated as a myelin sensitive and specific technique^{14–17}. The ihMT image is generated by the subtraction of a MT weighted image acquired with a single frequency irradiation (MT_{sing}) and one acquired with power evenly split between positive and negative frequency offsets (MT \pm)²⁴. In practice, to limit the effects of MT asymmetry⁴¹, the single frequency image MT_{sing} is obtained by adding an image at the positive frequency (MT₊) and one at the negative frequency (MT₋) such that

211 $MT_{\text{sing}}=MT_{+}+MT_{-}$. Hence, for consistency, the dual offset image is acquired twice such that
212 the ihMT image is given by $ihMT=(MT_{+}+MT_{-}-2MT_{\pm})$.

213 Several variants of the ihMT technique have been proposed in the past, including single slice
214 2D ihMT-HASTE (Half-Fourier Acquisition Single-shot Turbo spin Echo) for brain¹⁵ and
215 SC²⁴⁻²⁶; 3D ihMT-GRE for brain¹⁹ and multi-slice ihMT SE-EPI for SC^{27,42}. In this study,
216 a 3D ihMTRAGE sequence initially proposed for brain⁹, and recently adapted to cervical
217 spinal cord imaging^{43,44} was used. The preparation scheme (Table 1) was similar to^{9,21} and
218 used identically for both the brain and SC. Note however, that the spatial resolution and the
219 number of repetitions differed. IhMTsat metrics, corrected for T_1 -relaxation and B_1^{+} -
220 inhomogeneities that can bias regular ihMTR values (with ihMTR defined as $ihMT/2M_0$) at
221 $3T$ ^{44,45}, were derived based on a strategy recently customized for the ihMTRAGE framework
222 ²¹ (see 2.4 section).

224 2.3 Morphological measurements

225 Discal cross-sectional areas, as well as antero-posterior and right-left diameters of canal and
226 cord were manually measured by an experienced neurosurgeon for each subject using the
227 Horos software (horosproject.org), based on T_2 SPACE image (intra-rater reproducibility:
228 3.6%, 4.6%, 5.1%, 4.0%, 5.8%, and 7.6%, for canal AP diameter, canal RL diameter, SC AP
229 diameter, SC RL diameter, canal CSA, and SC CSA, respectively). Cord-to-canal (CCR) and
230 canal occupation (COR) ratios were subsequently derived (see definition in Table S1). The
231 degree of stenosis (see definition in Table 2) was assessed in the meantime using the same
232 contrast.

233 The axial T_2^{*} -weighted MGE images were used for the automatic segmentation of GM, WM,
234 and SC using the SCT⁴⁶ *deepseg* tool, from which mean CSAs were estimated at each level.
235 Finally, the UNI image (derived from MP2RAGE technique) was brain-extracted and
236 segmented into GM, WM, and cerebrospinal fluid (CSF) using SPM12
237 (<https://fil.ion.ucl.ac.uk/spm>) “*New segment*” tool⁴⁷. The volumes of brain GM and WM
238 were each normalized by the intracranial content (GM+WM+CSF) to remove inter-subject
239 differences and investigate variation with age.

2.4 T1 and ihMTsat post-processing

The post-processing steps to provide regional T_1 and ihMTsat measurements are depicted in Figure 1.

All MT-weighted volumes (MT_+ , MT_- , MT_\pm) of the ihMTRAGE images acquired on SC and brain were motion-corrected by SCT ⁴⁶ *MoCo* and *ihMT-MoCo* ⁴⁸, respectively. After motion correction, the MT-weighted volumes on SC and brain were registered to their respective T_1 maps using SCT *multi-modal registration* and SyN-ANTS ⁴⁹ rigid registration tools, respectively. As previously mentioned, the ihMTR ratio was not used in this study, instead the ihMTsat metric was calculated. The reader can refer to Munsch et al ²¹. Briefly, the derivation of ihMTsat approach ²¹ relies on a model that describes the effect of each RF saturation pulse as a fractional attenuation (δ) of the free water pool (e.g. the free pool magnetization right after a dual-offset RF pulse (MT_\pm') is related to the magnetization right before (MT_\pm) by $MT_\pm' = (1 - \delta_{MT_\pm}) \times MT_\pm$). B_1 and T_1 maps were used to determine the δ factors that fit the attenuation of each MT-w relative to the unsaturated M_0 image, given the ihMTRAGE sequence parameters. The ihMTsat metric was finally derived from the formulae ²¹:

$$ihMTsat = (2\delta_{MT_\pm} - \delta_{MT_+} - \delta_{MT_-}) \times \left(\frac{B_{1nom}}{B_{1act}} \right)^2,$$

Where the term $\left(\frac{B_{1nom}}{B_{1act}} \right)^2$ that accounts for the quadratic B_1 dependence of ihMT with the saturation parameters used ⁵⁰ corrects for B_1 inhomogeneities. B_{1nom} and B_{1act} represent the nominal and actual pulse amplitudes calculated from the B_1^+ map, respectively. The post-processing pipeline for ihMTsat maps derivation is available in: https://github.com/lsoustelle/ihmt_proc (hash f3f49e0).

The T_1 maps were then non-linearly registered to the ICBM-MNI-152^{51,52} template on brain and PAM50 template on SC⁵³. On SC, the PAM50 regions of interest including WM Corticospinal Tracts (CST), Lateral Sensory Tracts (LST), Posterior Sensory Tracts (PST), Rubro/Reticulospinal Tracts (RST), and anterior and intermediate GM (ant-int) were warped back into the subject space and used for quantification of the quantitative maps. On brain, in addition to WM and cortical GM compartments, deep GM structures including Thalamus, Nucleus Caudate, and Putamen were segmented using FSL *FIRST* tool (<https://fsl.fmrib.ox.ac.uk/>)⁵⁴. The brain maps were quantified for each of these compartments and deep GM regions.

2.5 Statistical analyses

The statistical analyses were performed using JMP Version 9 (SAS Institute Inc., Cary, NC). The mJOA and NDI scores were compared between the rugby players and controls using the non-parametric Steel-Dwass all pairs test, separately, and a p -value <0.05 was considered as statistically significant.

For SC, T_1 and ihMTsat parameters were compared between Rugby players and healthy controls using ANOVA, looking at the (R vs. HC) group effect when accounting for age and cervical levels. P values were corrected for multiple comparisons (5 ROIs, 2 parameters, $p_{\text{corrected}}<0.005$).

For the brain, T_1 and ihMTsat parameters were also compared between Rugby players and healthy controls in the three compartments using ANOVA, looking at the (R vs. HC) group effect when accounting for age. P values were corrected for multiple comparisons (3 compartments, 2 parameters, $p_{\text{corrected}}<0.008$).

To investigate the evolution of metrics with age, linear regressions were performed.

Finally, R_1 ($1/T_1$) and ihMTsat maps on brain and SC were used in voxel-wise multi-variate analyses using the Permutation Analysis of Linear Models (PALM) tool available in the FSL package (version alpha119)⁵⁶. The Non-Parametric Combination (NPC) option⁵⁵, which allows joint inference over multiple modalities, was more particularly used in this study. To benefit from the multi-parametric MR protocol, R_1 and ihMTsat maps were thus combined using NPC in order to locate potential tissue abnormalities and investigate whether R_1 and ihMTsat were significantly lower in players as compared to HC. For both brain and SC, the analysis was performed using WM mask, GM mask, and the whole structure. For the analysis, 5000 permutations were used, along with the Threshold Free Cluster Enhancement

(TFCE) option. The results were corrected for Family-Wise Error (FWEP-corrected) and for multiple modalities. The threshold was then set at $p\text{-value} < 0.05$.

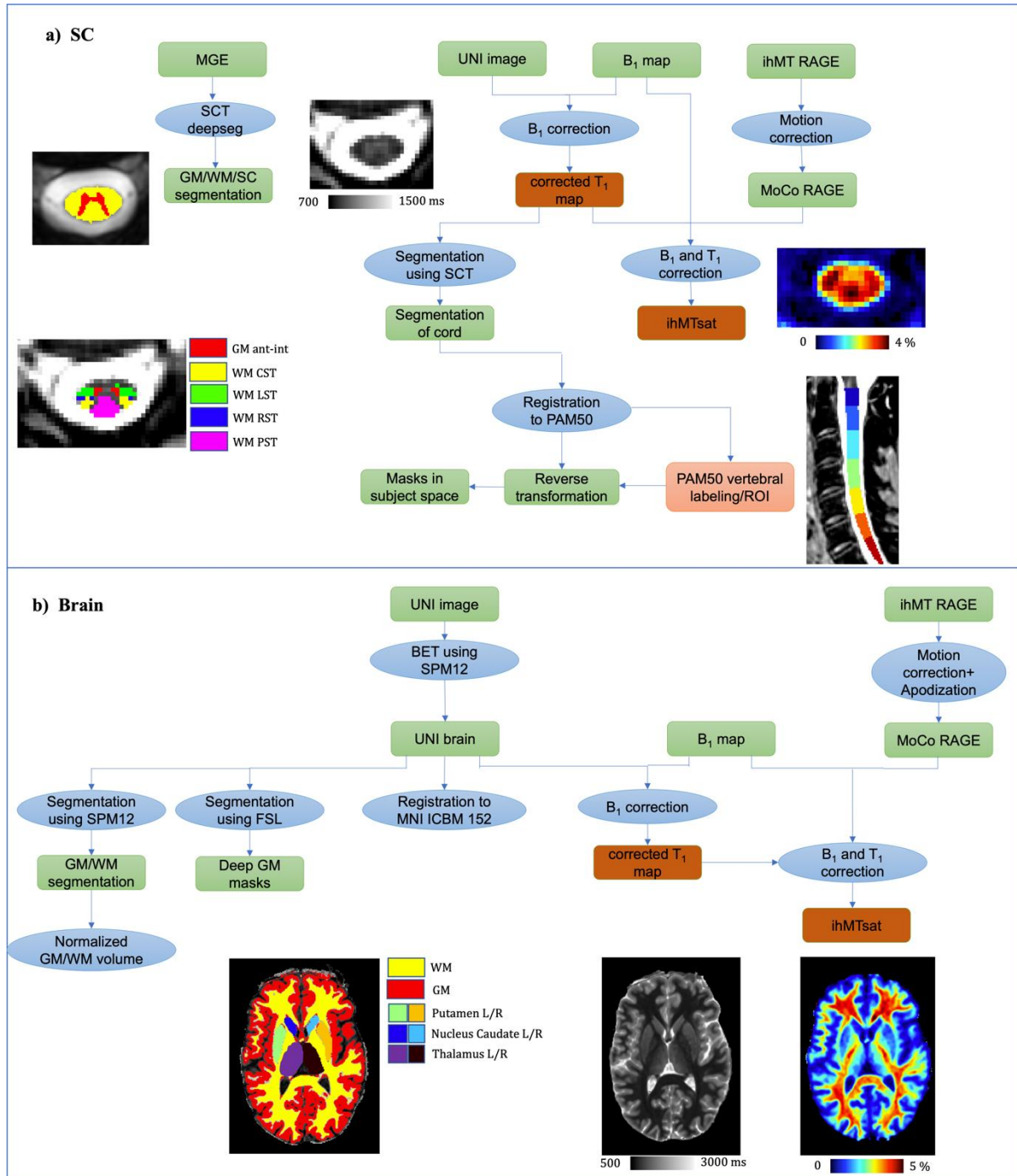


Figure 1: Main post-processing steps (motion correction, B_1^+ and/or T_1 bias-correction, registration and segmentation, ROI labeling) for MP2RAGE and ihMT images on both a) SC and b) brain. (ROIs on SC: GM ant-int: anterior and intermediate; WM CST: corticospinal tracts; LST: lateral sensory tracts; RST: rubro/reticulospinal tracts; PST: posterior sensory tracts).

2.6 Data/code availability statements

Data can be made available via a request to the authors and will be shared through a formal data sharing agreement.

The post-processing code has been well described in the Materials & Methods section and Figure 1, with all the software and toolboxes used (SCT, FSL, SPM, ANTS, etc.). The ihMTsat map derivation code is also available at: https://github.com/lsoustelle/ihmt_proc (hash f3f49e0)).

3 Results

3.1 Clinical assessment

All scores are summarized in Table 2. All rugby players and 13 HC presented at least one grade of canal stenosis. NDI were significantly higher in players than in controls (p -value <0.005), but with values ranging from normal to mild disability. No significant differences were observed between the mJOA scores of players and HC, however, 3 amateur players presented mild alterations.

	Retired Rugby Players (R)	Healthy controls (HC)
Number of participants	15	15
Players in front / second / third row position	8 / 4 / 3	-
Mean age (years old (yo)) [min, median, max]	46.8 \pm 7.6 [34, 46, 62]	48.6 \pm 9.5 [37, 47, 71]
Mean rugby practice duration (yo)	26.2 \pm 9.5	-
Mean duration from rugby practice retirement (yo)	9.8 \pm 5.4	-
Clinical scoring		
mJOA (/17)	16.7 \pm 0.5	17
NDI (%) [min, median, max]	9.4\pm7.2 ** [0, 8, 30]	4\pm8.7 [0, 0, 34]
OSS [min, median, max]	1.8 \pm 0.8 [1, 2, 3]	1.9 \pm 1.1 [0, 2, 4]
<i>mJOA, from 0 to 17, with values between 15 to 17 considered as mild degeneration and ≤ 14 as moderate-to-severe²⁸; NDI, from 0 to 50; also expressed from 0 to 100%, with values $<8\%$, $< [10-28\%]$, and $[30-48\%]$ considered as normal, mild and moderate disability, respectively²⁹; OSS, from 0 to 18, defined as the sum of stenosis score at each level (C2-3 to C6-C7 and C1) in a range of 0 to 3 for normal, mildly, moderately, or severely compressed, respectively.</i>		

Table 2: Demographic data, NDI and mJOA scores, and overall stenosis score (OSS); **: p -value <0.01 .

3.2 Morphological results

Morphological results are summarized in table S1 (supplementary data). No differences in SC and brain morphometrics were observed between rugby players and healthy controls. However, for cerebral GM compartment, one age×group interaction was observed (ANOVA $p<0.03$) related to a significant negative correlation between normalized GM volume and age in rugby players ($p=0.003$), not observed in controls. (Figure 2a).

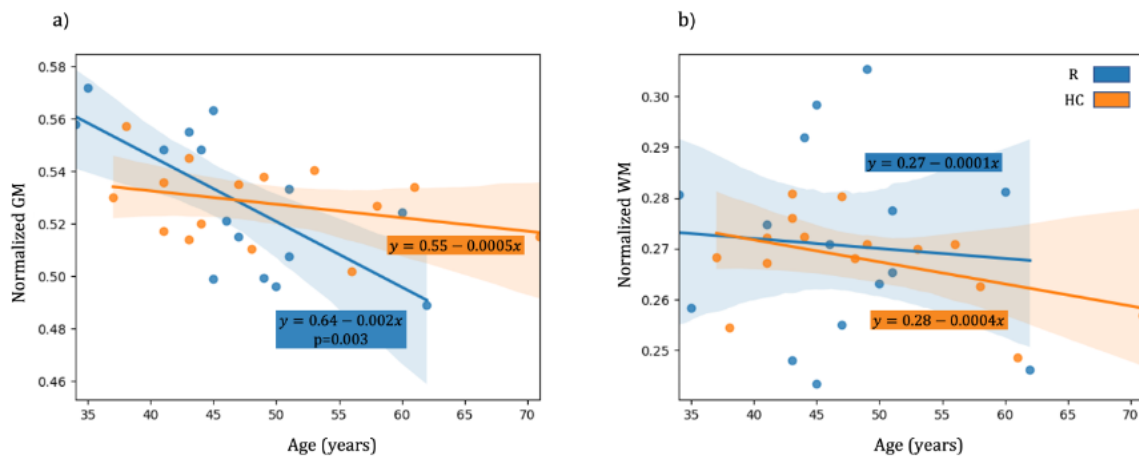


Figure 2: Regression plots for (a) Normalized GM and (b) Normalized WM (on brain) volumes vs. age, for Rugby players (R, blue) and Healthy Controls, (HC, orange). Age had a significant effect on the normalized GM volume in the rugby players group ($p=0.003$) that was not observed in HC, nor in WM.

3.3 Quantitative imaging results

Representative images and quantitative T_1 and ihMTsat maps of both brain and SC obtained from one rugby player are provided on Figure 3.

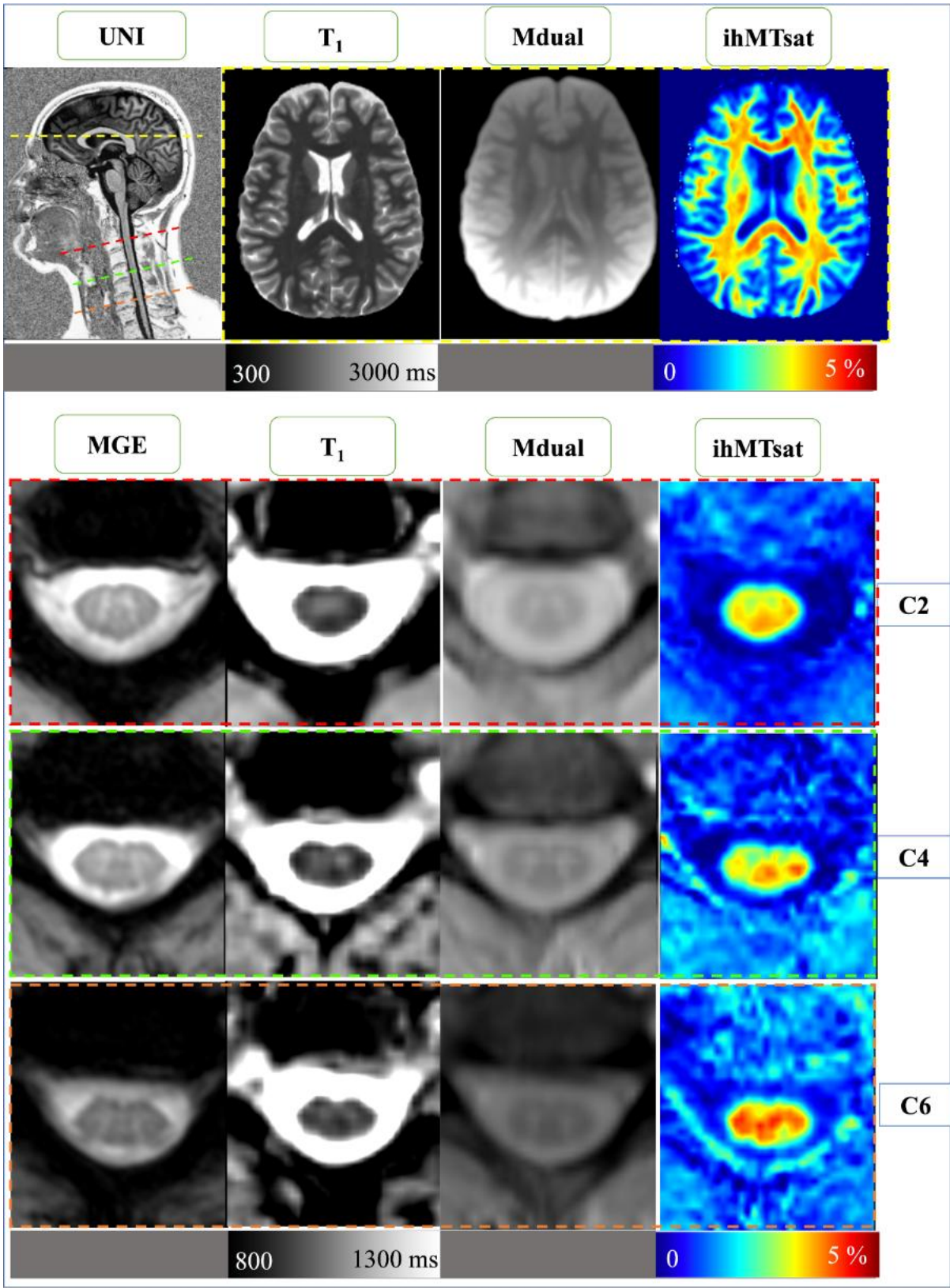


Figure 3: Representative SC and brain images acquired on one retired rugby player (top: sagittal UNI MP2RAGE showing both brain and cervical cord; axial quantitative T_1 map, axial MT weighted image obtained with a dual-offset saturation (MT_{dual}) and corresponding ihMTsat acquired mid-brain; bottom: axial T_2^* -weighted MGE, T_1 map, MT_{dual} and ihMTsat acquired at C2, C4 and C6 levels).

IhMT data biased from PVE due to cord curvature (visual assessment) were removed from the analysis (2, 2, 8, and 9 images for the C1, C2, C6, and C7 levels, respectively, for rugby players and 1, 1, 1, 7 and 8 images at C1, C2, C5, C6, and C7 levels for the HC). Brain ihMTsat maps of one rugby player and one HC were also removed because of motion artifacts. Conversely, brain and SC T_1 maps of all subjects were kept.

Mean maps of R_1 ($1/T_1$) and ihMTsat for both rugby players and HC groups (obtained by averaging all individual maps co-registered in the PAM50 and MNI-152 template spaces) are presented on Figure 4. Rugby players globally presented with lower R_1 (i.e. higher T_1) on SC, and a trend toward lower R_1 and ihMTsat on brain.

Mean T_1 and ihMTsat values in the different ROIs are summarized on table 3 for both brain and cord, and for the 2 groups. On all ROIs of SC, the T_1 values were significantly higher in players as compared to HC. No significant differences were observed on brain. Detailed values of the 2 metrics in various brain regions derived from ICBM-MNI-152 lobes atlas^{51,52} and JHU ICBM-DTI-81 WM label atlas^{57,58} are provided in Table S2 (supplementary data) for reference and readers who might be interested, but none of them reached statistical significance.

qMRI		T_1 (ms)		ihMTsat (%)	
SC ROI		R	HC	R	HC
WM	CST	929.7±26.5*	917.3±25.7	3.2±0.1	3.2±0.2
	PST	953.5±27.6	941.1±33	3.3±0.2	3.3±0.3
	RST	919±25.1***	901.4±25.2	3.2±0.1	3.2±0.2
	LST	925±34.2*	911.9±27.7	3.1±0.2	3.1±0.2
GM	ant-int	978.7±23.3*	967.6±19.5	3.0±0.1	3.0±0.2
Brain ROI					
WM		830.8±17.3	817.9±21.6	3.3±0.1	3.4±0.1

GM	1315.3±26.8	1307.7±19.1	1.2±0.1	1.2±0.1
dGM	1130.7±28.2	1130.1±29.7	1.4±0.1	1.4±0.1

Table 3: The mean \pm inter-subject SD of T_1 and ihMTsat in rugby players (R) and healthy controls (HC) in different ROIs of SC and brain (see Figure 1). *: p -value<0.05, ***: p -value<0.001. The p -values correspond to the MANOVA test performed on each ROI and corrected for multiple analyses (different ROIs, 2 parameters) on brain and SC, separately.

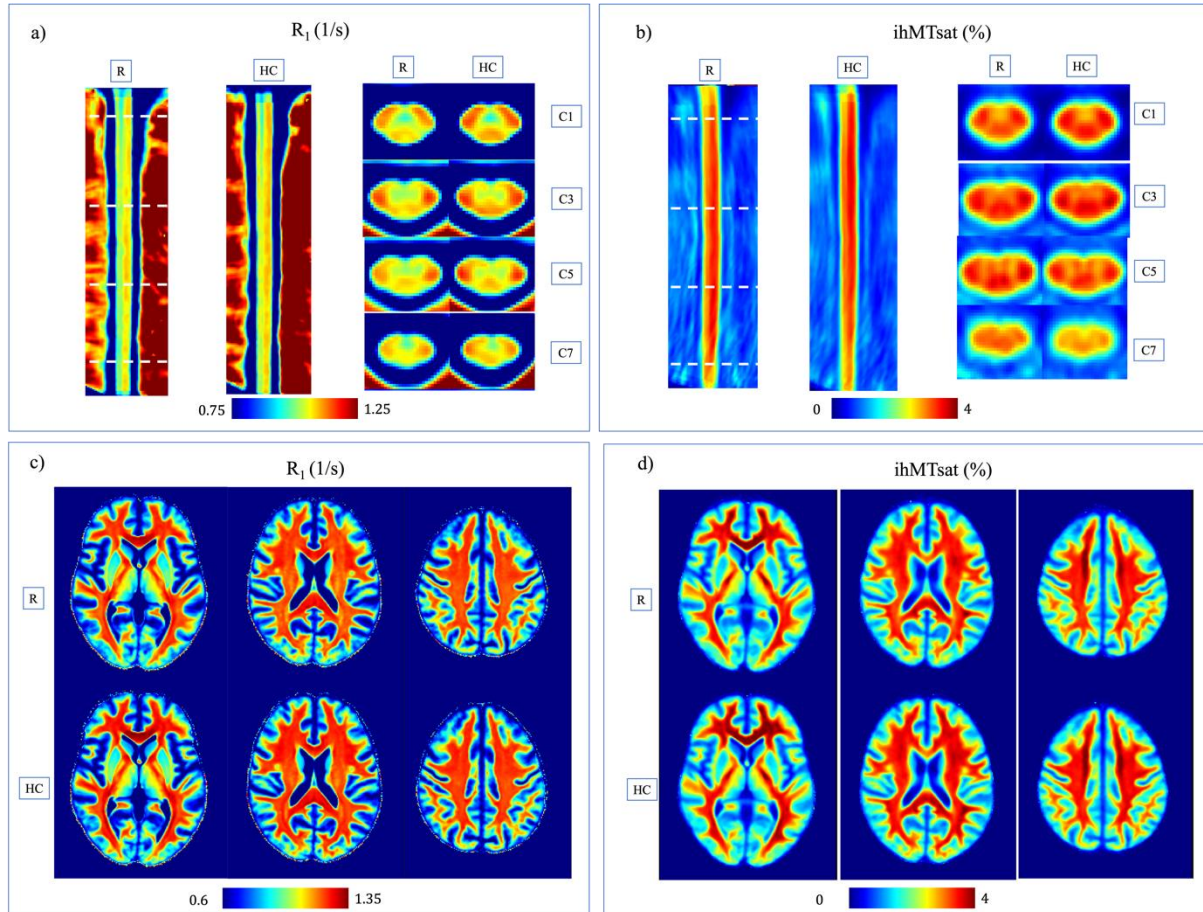
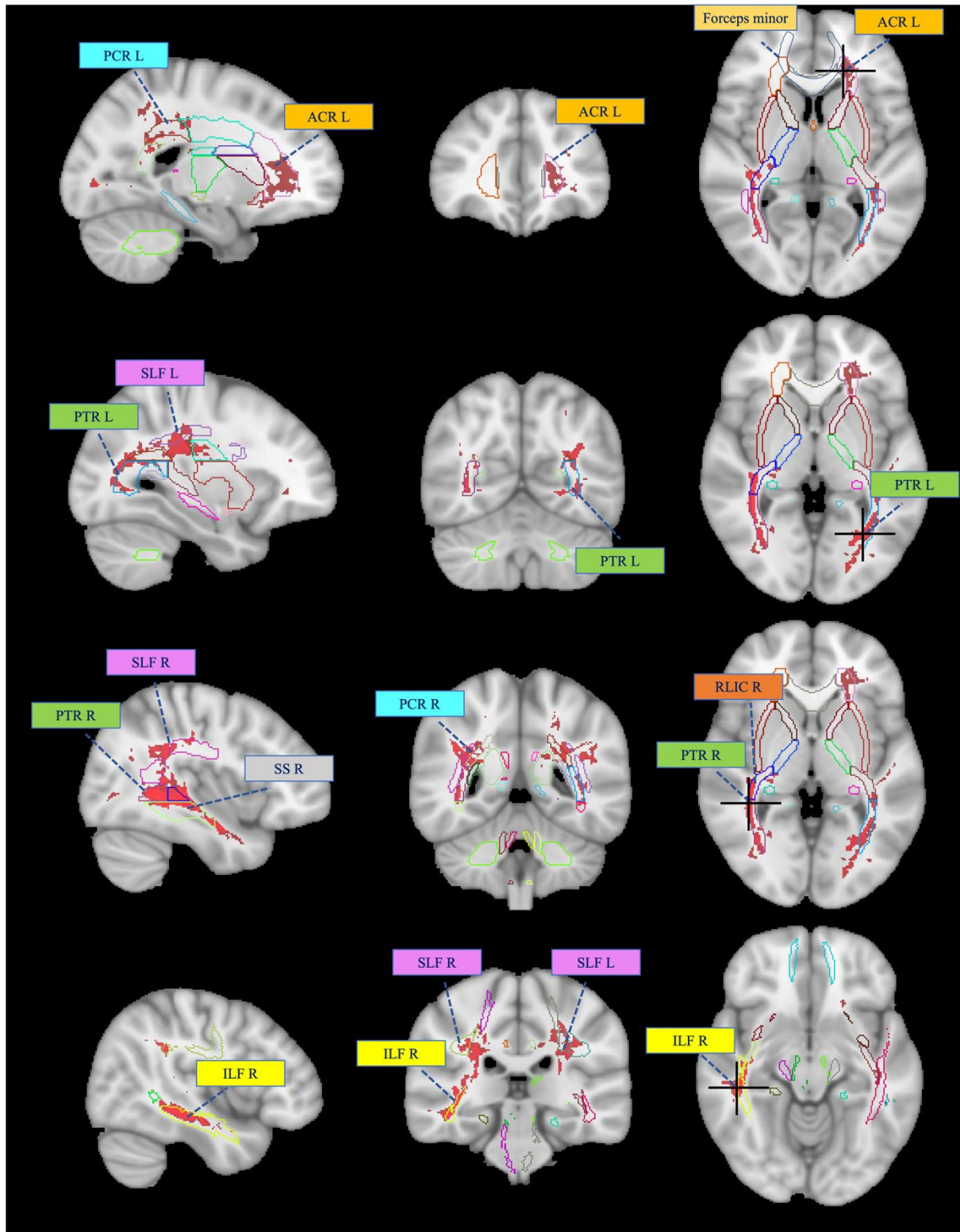


Figure 4: (a) Mean R_1 ($1/T_1$) maps on SC, (b) mean ihMTsat maps on SC, (c) mean R_1 maps on brain, (d) mean ihMTsat maps on brain, for the 15 rugby players and 15 HC (sagittal and axial planes on SC, presented in the PAM50 space and axial planes on brain presented in MNI-152 template).

Figure 5 shows the clusters obtained by the PALM multi-variate test (with R_1 and ihMTsat metrics and using brain WM mask), in which a significant decrease in R_1 and/or ihMTsat was observed in players as compared to controls. Labels of tracts in which the clusters are located were derived from the JHU white-matter tractography⁵⁹ and ICBM-DTI-81 white-matter labels atlases^{57,58}. The same tests were done with GM mask on brain, and GM and WM masks on SC, but no significant clusters were found.



380

381 *Figure 5: Identification of the WM tracts where significant clusters from the PALM multi-variate analysis of R_1*
 382 *and ihMTsat are located. The atlases used for cluster localization are JHU white-matter tractography⁵⁹ and*
 383 *ICBM-DTI-81 white-matter labels atlases^{57,58}. The ROIs illustrated here are: ACR L: Anterior Corona Radiata*
 384 *L; PCR R/L: Posterior Corona Radiata Right/Left; RLIC R: Retrolenticular Limb of Internal Capsule; PTR R/L:*
 385 *Posterior Thalamic Radiation Right/Left; SLF R/L: Superior Longitudinal Fasciculus Right/left; SS R: Sagittal*
 386 *Stratum R; ILF R: Inferior Longitudinal Fasciculus Right; and Forceps minor.*

387

388

389 Finally, the linear regression plots of T_1 and ihMTsat values with age in different ROIs of
390 brain and SC are given in Figure 6. As shown from HC values (orange lines), T_1 increased
391 with age in the normal population with statistical significance in brain WM regions (Fig. 6d,
392 $p=0.0006$), and ihMTsat decreased in brain WM (Fig. 6h, $p=0.003$) and SC WM and GM
393 regions (Fig. 6e and 6g, $p\leq 0.02$). Different behaviors were observed for rugby players (blue
394 lines): T_1 decreased slightly with age in SC GM (Fig. 6a) and brain WM (Fig. 6d), and
395 significantly in brain GM (Fig. 6b, $p=0.02$), with all initial values above those of HC. For
396 ihMTsat, all initial values were below those observed in HC, values then remained fairly
397 constant with age in brain and SC GM (Fig. 6e and 6f), and slightly decreased in brain and
398 SC WM (with a slope almost divided by 2 as compared to HC, Fig. 6g and 6h).

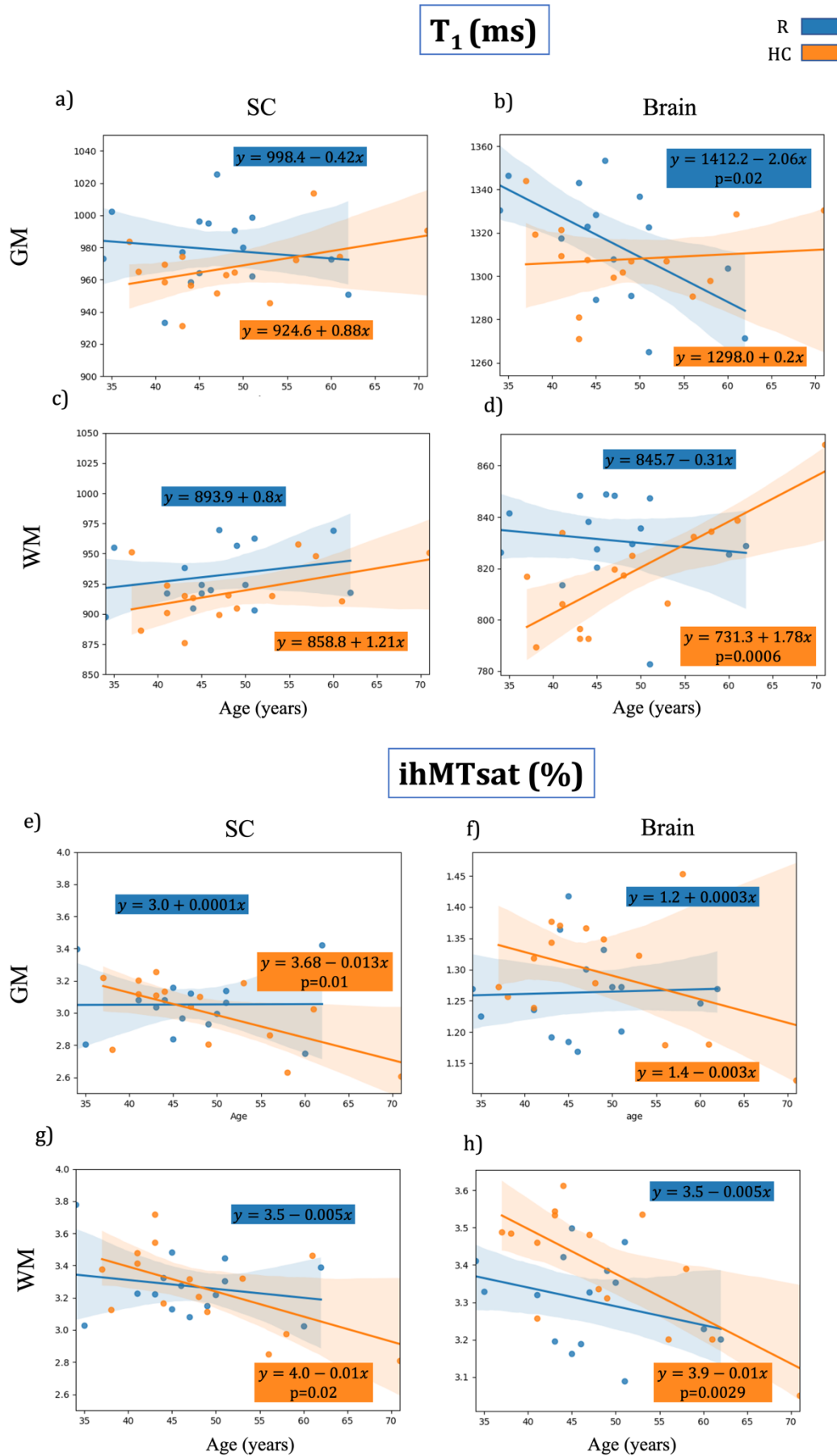


Figure 6: Linear regression plots and equations (along with MANOVA p-value if <0.05) for evolution of T_1 and ihMTsat with age in GM and WM of brain and SC in R (blue) and HC (orange). The T_1 in brain and SC GM decreased for rugby players with age, contrary to HC (a, b). In brain WM of rugby players, a decrease of T_1 with age together with a moderate decrease of ihMTsat as compared to HC can also be observed (d, h). Finally, values of ihMTsat in brain and SC GM remained fairly stable with age for rugby players whereas they tend to decrease for HC. GM in brain corresponds here to the whole cortical GM; WM in SC includes PST, CST, LST, and RST regions.

4 Discussion

While spine degeneration linked to rugby activity has been previously reported ^{6,7}, little is known about the spinal cord itself. Taking advantage of a multi-parametric MR protocol including quantitative state-of-the-art T_1 MP2RAGE and ihMT techniques, both spinal cord and brain tissues from retired rugby players were analyzed in an attempt to characterize possible early aging and to refine tissue damage description. The global observations made between players and HC are summarized in Table 4. While brain and spine morphometrics were not largely affected in this population of retired rugby players, microstructure tissue damage was demonstrated, with deleterious effect of potential cumulative microtrauma highlighted with the multivariate voxel-wise approach, especially on cerebral WM tracts.

Metrics	Global observations	Statistical significance	Pathophysiological hypothesis / Comments
Brain qMRI			
Multi-variate analysis using R_1 ($1/T_1$) and ihMTsat in brain WM;	Lower R_1 (higher T_1) and lower ihMTsat for players as compared to HC, in various regions such as ACR L, PCR R/L, RLIC R, PTR R/L, SLF R/L, SS R, GCC, BCC, ILF R, and Forceps minor	$p < 0.05$	Degeneration and demyelination in these specific WM tracts
T_1 in GM	Significantly decreases with age in players	$p = 0.02$	Potential iron accumulation due to micro-hemorrhages induced by repetitive impacts
T_1 in WM	Significantly increases with age in HC but not players Initial values for players above those	$p = 0.0006$	Early aging followed by potential iron accumulation or restructuration processes

	observed in HC		
ihMTsat in WM	Significantly decreases with age in HC but not in players Initial values for players below those observed in HC	p=0.003	Early aging followed by restructuration potentially involving microglia
SC qMRI			
Mean T ₁ in SC GM and WM	Higher T ₁ for players as compared to HC	p<0.05	Diffuse degeneration in the cord, but not necessarily due to demyelination
Mean ihMTsat in SC GM and WM	Similar range in average	No	
Clinical/Morphological assessment of Spine			
Cord-to-canal ratio (CCR)	Higher trend for players on all levels (0.62 on average)	No	Slight degenerative cervical spine (without specific cord atrophy) in the range of higher risk of trauma or chronic degenerative abnormalities ^{6,60}
NDI	Higher in players than HC, but ranging from normal to mild disability	p=0.005	Higher CCR but normal/mild disability in favor of efficient muscle strengthening programs and higher pain threshold in players ⁷

Table 4: Summary of all the global observations and differences between the players and HC.

4.1 Clinical scoring and morphological variations

Previous studies on the cervical spine of former professional rugby players showed that players complained of chronic neck pain significantly more than controls, with more foraminal stenosis, narrower AP cord diameter, higher CCR, but no significant difference for clinical evaluations (JOA questionnaire, visual analog scale and NDI) ^{6,7}. Results from the present study, performed on a much smaller cohort, globally aligned with these observations (significantly higher NDI but ranging from normal to mild, slightly different AP diameter, canal stenosis, and higher CCR), nonetheless spine degeneration was not prominent in this population.

On the brain, cortical and cerebellar GM volumes were showed to reduce with age in the normal population ^{61,62}. Here, the reduction in brain GM volume with age happened at a significantly faster rate for rugby players, which could indicate an early aging effect in brain GM linked to the rugby practice. However, the mean brain GM volume did not significantly

differ between players and controls, thus requiring further study on larger cohorts and time points to better understand the tissue dynamic.

4.2 Quantitative MR metrics alterations

The potential microstructural alterations of the SC in players of contact sports have never been studied before, except in a preliminary investigative study relying on MP2RAGE and DTI that reported altered T_1 and DTI metrics in players ($n=4$), especially in levels with disc protrusion⁶³. In our study and for the first time, these potential alterations were more largely investigated using both T_1 and ihMTsat. The higher T_1 values in GM and WM cSC regions observed in retired rugby players as compared to HC could demonstrate a diffuse microstructural alteration occurring as a result of rugby practice. However, the lack of difference in ihMTsat values between players and HC may indicate that the alterations are not necessarily related to demyelination or that alterations seen with ihMTsat could not be caught with the same sensitivity as in T_1 . Future studies should focus on the sensitivity of each technique. It would also be interesting to combine MR investigation with biomechanical simulations⁶³ to further understand the effects of repetitive impacts on the spinal cord tissue and the presence of damage despite non prominent spine degeneration.

On brain, different studies have investigated the effects of sub-concussive impacts in athletes of contact sports. DTI and fMRI are among the tools commonly used to study these effects^{5,64}. It was previously shown that football players demonstrated changes in their default mode network pre-season and post-season⁶⁵, and that there was a relationship between age at first exposure to football and the white matter microstructure in professional players, which resulted in significant changes in DTI measures such as lower fractional anisotropy (FA) and higher radial diffusivity (RD) in anterior regions of corpus callosum⁶⁴. One DTI study on ice hockey players also found that axial diffusivity (AD) and RD values in the right precentral region, right corona radiata, the anterior and posterior limb of the internal capsule and the superior longitudinal fasciculus were significantly different pre- and post-season⁶⁶. Whereas these studies demonstrate the more acute and short-term effects of alterations in players of contact sports, our voxel-wise multi-variate analysis using both R_1 and ihMTsat showed significant clusters in identical brain regions such as corona radiata, internal capsule, superior and inferior longitudinal fasciculus, which could additionally indicate long term or persistent abnormalities that may be linked to the accumulating effect of impacts encountered in the

rugby practice. The means of T_1 and ihMTsat in different ROIs of brain (table S2) show a similar (but non-significant) trend.

We also observed a significant decrease of T_1 with aging in brain GM of rugby players that could be indicative of excessive iron accumulation (together with a non-significant trend in SC GM). Iron is essential for a normal functioning brain, however impaired regulation can result in the production and accumulation of reactive oxygen species and cause oxidative stress that the biological system is not able to detoxify^{67,68}. Iron accumulation occurs in brain GM with normal aging^{69,70}, however, there is a growing body of evidence that repetitive impacts can result in microhemorrhages and consequently, excessive iron deposition⁶⁸. In parallel, excessive iron deposition has been reported in several neurodegenerative diseases such as PD^{71,72}, MS⁷³, and Amyotrophic Lateral Sclerosis (ALS)^{74,75} and recent studies demonstrate that contact sports that involve repetitive head and cervical spine impacts, such as soccer and American football, could be a risk factor for ALS^{76,77}. Nonetheless, further studies using techniques sensitive to iron such as quantitative susceptibility mapping (QSM)⁷⁸ would be required to further validate this hypothesis.

Finally, when investigating the aging effect on ihMTsat values of rugby players, we observed an early decrease (in younger players as compared to HC) that could indicate demyelination and early degeneration, however, values in GM and WM then did not decrease with age as in HC, which may be linked to tissue restructuration involving microglia for instance⁷⁹. Indeed, the ihMT technique is supposedly myelin specific, however, a recent study demonstrated that ihMTsat obtained with cosine-modulated RF pulses for the dual-offset saturation (as in here) is less specific to myelination than approaches using frequency-alternated RF pulses, because non-myelin macromolecules, presumably associated with glial cells, also contribute to the ihMTsat signal⁸⁰. Here, microglia could thus significantly contribute to the ihMTsat value, hence counteracting the expected decrease of ihMTsat with age as a consequence of myelin loss with age. Further studies should consider this methodological aspect to possibly disentangle the different pathophysiological mechanisms.

4.3 Limitations & Perspectives

This exploratory study was performed on a retired group of rugby players and the HC group was selected to match the age of players but other parameters such as profession, lifestyle, or hours of sports practice were not considered. More importantly, this investigative study was conducted on a limited number of participants and the effects should now be investigated in a

larger cohort of players. Analyses based on the players experience in professional or amateur leagues could not be considered in this study due to statistical power, but similar trends were observed for both sub-populations in the cohort (data not shown). This would nonetheless require further investigations. The position of the players (forwards, especially front row, vs. backs) could not be considered either due to statistical power, but such distinction would be interesting in the future. Furthermore, a longitudinal study over time and different playing seasons would allow to better delineate the short- and long-term effects of impacts. Recording impacts information such as force, moment, and linear and rotational accelerations as in ⁸¹⁻⁸³ would additionally enable to investigate the correlation between biomechanical forces of impacts and MRI indices of structural integrity and should be considered in the future.

Another technical limitation of this study was the spatial resolution of the ihMT technique for spinal cord imaging. The slice thickness was 10 mm to maximize SNR while keeping the acquisition time clinically acceptable (~10 min). This made the sequence prone to partial volume effect when the cord is curved (and some data had to be discarded at the lower levels of the cord) and potentially less sensitive to very focal abnormalities (which were nonetheless not necessarily expected here). Note that the TR (2500 ms) could have been decreased in a normal context to accelerate the acquisition time, however, the morphology of the rugby players precludes such adjustment to stay within specific absorption rate (SAR) guidelines. This should be further improved in future developments.

One should also keep in mind that the MP2RAGE technique estimates the T_1 of the tissue based on the UNI image obtained from the two RAGE volumes acquired with 2 different TIs. Although T_1 values obtained from MP2RAGE techniques have been previously validated in phantom against IR-SE ³⁸, and against values reported in literature for different brain and SC regions ⁸, it is not a pure measurement of the T_1 .

As mentioned in the above section, it would also be interesting to work with a frequency-alternated RF pulses ihMT sequence and combine this technique with a QSM approach in order to disentangle the different possible pathophysiological hypotheses that have been raised in this study.

Despite some limitations, and to the best of our knowledge, this study is the first to characterize cord tissue alterations in players of contact sports using quantitative MR techniques. This study is also the first investigating both brain and cSC microstructural alterations at the same time with T_1 MP2RAGE and ihMT-RAGE techniques.

The techniques and post-processing tools developed in this study can now be further used to investigate microstructural alterations in other contact sports, different CNS pathologies or aging in general.

5 Conclusion

In this work, retired professional and amateur rugby players and age-matched healthy controls were recruited and studied for potential microstructural alterations of both brain and cSC using medical questionnaires and qualitative and quantitative MR techniques including T_1 relaxometry and ihMT sequences.

Higher NDI scores, higher cord-to-canal ratio, higher T_1 values suggestive of structural degeneration of cSC, together with increased T_1 and decreased ihMTsat suggestive of brain demyelination have been observed in retired rugby players as compared to age-matched controls, potentially due to cumulative effect of long-term impacts. Measurements also suggest early aging and different aging processes on brain in the players. These preliminary observations provide new insights, which should now be further investigated on larger cohorts and multicentric longitudinal studies and further correlated to the likelihood of neurodegenerative diseases^{68,71–75} and risk factors.

Acknowledgements

This work was performed within a laboratory member of France Life Imaging network (grant ANR-11-INBS-0006) and was supported by the Institut Carnot Star, the ARSEP Foundation (Fondation pour l'Aide à la Recherche sur la Sclérose en Plaques) and the CNRS (Centre National de la Recherche Scientifique). The project also received funding from the European Union's Horizon 2020 research and innovation program under the Marie Skłodowska-Curie grant agreement No713750, with the financial support of the Regional Council of Provence-Alpes-Côte d'Azur and A*MIDEX (n° ANR-11-IDEX-0001-02), funded by the Investissements d'Avenir project funded by the French Government, managed by the French National Research Agency (ANR).

The authors would like to thank T. Kober from Siemens Healthcare for MP2RAGE sequence support, A. Massire for T_1 post-processing code support, as well as V. Gimenez, C. Costes, P. Viout, L. Pini and MP. Ranjeva for study logistics.

565

566

MORPHOLOGICAL DATA ON BOTH SPINAL CORD & BRAIN											
Spinal cord	CCR		COR		CSA (mm ²)						
						SC		GM		WM	
Discal level	R	HC	R	HC	Vertebral level	R	HC	R	HC	R	HC
C1	0.53±0.05	0.50±0.06	0.28±0.05	0.25±0.03	C1	76.4±5.6	77.2±8.1	15.7±1.5	15.3±1.5	60.7±4.3	61.8±7.1
C2-C3	0.66±0.06	0.64±0.07	0.37±0.06	0.34±0.03	C2	76.2±5.7	76.5±8.4	15.0±1.0	14.5±1.2	61.3±5.2	61.9±7.4
C3-C4	0.65±0.07	0.64±0.07	0.44±0.07	0.45±0.06	C3	76.2±6.4	76.4±8.7	15.3±1.6	15.6±1.2	60.9±4.9	60.8±7.7
C4-C5	0.63±0.07	0.61±0.06	0.45±0.07	0.44±0.06	C4	81.1±6.5	79.3±8.6	17.8±1.9	18.2±2.1	63.3±5.4	61.1±6.8
C5-C6	0.64±0.07	0.62±0.07	0.47±0.05	0.48±0.07	C5	78.7±7.4	77.4±11.2	17.2±2.3	17.6±2.3	61.4±5.6	59.8±9.1
C6-C7	0.61±0.09	0.60±0.06	0.41±0.08	0.43±0.05	C6	69.2±5.4	70.9±12.4	15.5±1.9	15.6±3.3	53.7±4.3	55.3±10.0
-	-	-	-	-	C7	58.1±6.5	59.4±12.8	12.4±1.8	11.0±3.8	44.9±7.2	47.2±13.7
Mean±SD	0.62±0.08	0.60±0.08	0.40±0.09	0.40±0.09	Mean±SD	73.7±9.4	73.9±11.8	15.5±2.3	15.4±3.2	58.0±8.0	58.3±10.2
Brain	Normalized GM (%)						Normalized WM (%)				
	R		HC			R		HC			
Mean±SD	52.8±1.4		52.8±2.7			26.7±0.9		27.0±1.8			

569 Table S1: Morphological measurements (mean ± inter-subject SD) on SC and brain for rugby players (R) and
570 HC: cord-to-canal ratio (CCR= $\varnothing_{AP_SC}/\varnothing_{AP_canal}$), canal occupation ratio (COR= $dCSA_{SC}/dCSA_{canal}$) and cord
571 cross sectional area (CSA), with \varnothing_{AP_SC} and \varnothing_{AP_canal} the antero-posterior (AP) diameters of cord and canal,
572 respectively, and $dCSA_{canal}$ and $dCSA_{SC}$, the canal and cord cross-sectional areas measured at each discal level
573 (C2-3 to C6-7 and C1 vertebral level). Discal cross-sectional areas and right-left (RL) or AP diameters are not
574 reported here but could be provided upon request. No statistical differences were observed between rugby
575 players and healthy controls except for \varnothing_{AP_canal} on C2-C3 (R vs. HC: 12.0±0.9 mm vs. 12.8±1.2 mm; p-
576 value<0.05) and \varnothing_{RL_canal} on C1 (R vs. HC: 22.5±2.2 mm vs. 24.3±1.8 mm; p-value<0.05).

577

578

QUANTITATIVE DATA ON SPECIFIC AREAS OF THE BRAIN					
		T1 (ms)		ihMTsat (%)	
Brain ROI		R	HC	R	HC
GM	Frontal	1285.3±32.8	1279.3±23.2	1.4±0.1	1.4±0.1
	Parietal	1269.1±30.9	1262.7±22.3	1.3±0.1	1.3±0.1

	Occipital	1283.4±30.1	1277.9±20.9	1.2±0.1	1.2±0.1
	Temporal	1388.8±34.8	1379.6±22.8	1.2±0.1	1.2±0.1
dGM	Thalamus	1195.7±30.3	1200.3±32.8	1.1±0.1	1.1±0.1
	Putamen	1142.1±31.3	1139.9±28.4	1.3±0.1	1.4±0.1
	Nucleus Caudate	1054.3±25	1049.9±36.8	1.8±0.1	1.8±0.1
WM Tracts	Corpus Callosum (CC) Genu	790.7±16.7	777.9±23	3.5±0.5	3.7±0.2
	CC Body	813.5±15.9	800.8±20.9	3.1±0.4	3.3±0.1
	CST	903.9±17.2	900.7±21	3.3±0.2	3.3±0.2
	Retrolenticular part of internal capsule R	811.2±20.8	794.9±20.9	3.1±0.4	3.4±0.2
	Anterior Corona Radiata R / L	818.3±21.3/ 816.9±20.9	800.1±24.8/ 798.8±24.1	3.4±0.5/ 3.4±0.4	3.6±0.2/ 3.7±0.1
	Posterior Corona Radiata R / L	845±19.2/ 846.7±16.6	823.4±32.7/ 825.3±30.8	3±0.4/ 3.1±0.4	3.3±0.2/ 3.4±0.2
	Posterior Thalamic Radiation R/ L	822.4±23.3/ 817.9±20.8	796.9±33.5/ 794±30.7	3.2±0.4/ 3.2±0.4	3.4±0.2/ 3.6±0.2
	Sagittal Stratum R/ L	832±20.8/ 837.4±17.7	806.9±23/ 819±22.9	3±0.4/3.1±0.4	3.3±0.2/ 3.2±0.2
	External Capsule R/L	848.4±22.2/846.9±21.7	832.3±22.3/832±21.7	3.1±0.1/3.1±0.4	3.2±0.1/3.3±0.1
	Cingulate Gyrus R/ L	804.3±20.1/797.6±18.8	790.7±22.1/784.4±20.4	3±0.4/ 3.1±0.4	3.2±0.1/ 3.2±0.2
	Fornix R	827.8±23.6	818.9±23.7	2.7±0.3	2.9±0.1
	Tapetum R / L	877.2±34.1/867.7±30.4	843.9±28/ 837.3±24.6	2.5±0.4/ 2.5±0.4	2.7±0.2/ 2.8±0.2

Table S2: Mean±SD (inter-subject) for T_1 and ihMTsat in different brain WM and GM ROIs for rugby players (R) and healthy controls (HC). No statistical differences could be observed, although some ROIs presented a trend for higher T_1 and lower ihMTsat for rugby players, also seen on Figure 4.

References

1. Bathgate A, Best JP, Craig G, Jamieson M. A prospective study of injuries to elite Australian rugby union players. *Br J Sports Med.* 2002;36(4):265-269. doi:10.1136/bjsm.36.4.265
2. Shuttleworth-Rdwards AB, Radloff SE. Compromised visuomotor processing speed in players of Rugby Union from school through to the national adult level. *Arch Clin Neuropsychol.* 2008;23(5):511-520. doi:10.1016/j.acn.2008.05.002
3. Alexander DG, Shuttleworth-Edwards AB, Kidd M, Malcolm CM. Mild traumatic brain injuries in early adolescent rugby players: Long-term neurocognitive and academic outcomes. *Brain Inj.* 2015;29(9):1113-1125. doi:10.3109/02699052.2015.1031699
4. Hume PA, Theadom A, Lewis GN, et al. A Comparison of Cognitive Function in Former Rugby Union Players Compared with Former Non-Contact-Sport Players and the Impact of Concussion History. *Sport Med.* 2017;47(6):1209-1220. doi:10.1007/s40279-016-0608-8
5. Manning KY, Brooks JS, Dickey JP, et al. Longitudinal changes of brain microstructure and function in nonconcussed female rugby players. *Neurology.* 2020;95(4):E402-E412. doi:10.1212/WNL.00000000000009821
6. Berge J, Marque B, Vital JM, Sénégas J, Caillé JM. Age-related changes in the cervical spines of front-line rugby players. *Am J Sports Med.* 1999;27(4):422-429. doi:10.1177/03635465990270040401
7. Brauge D, Delpierre C, Adam P, Sol JC, Bernard P, Roux FE. Clinical and radiological cervical spine evaluation in retired professional rugby players. *J Neurosurg Spine.* 2015;23(5):551-557. doi:10.3171/2015.1.SPINE14594
8. Forodighasemabadi A, Rasoanandrianina H, El Mendili MM, Guye M, Callot V. An optimized MP2RAGE sequence for studying both brain and cervical spinal cord in a single acquisition at 3T. *Magn Reson Imaging.* 2021;84(September):18-26. doi:10.1016/j.mri.2021.08.011
9. Varma G, Munsch F, Burns B, et al. Three- dimensional inhomogeneous magnetization transfer with rapid gradient- echo (3D ihMTRAGE) imaging. *Magn Reson Med.* 2020;(April):mrm.28324. doi:10.1002/mrm.28324
10. Haacke EM, Cheng NYC, House MJ, et al. Imaging iron stores in the brain using

magnetic resonance imaging. *Magn Reson Imaging*. 2005;23(1):1-25.

doi:10.1016/j.mri.2004.10.001

11. Sian-Hülsmann J, Mandel S, Youdim MBH, Riederer P. The relevance of iron in the pathogenesis of Parkinson's disease. *J Neurochem*. 2011;118(6):939-957.

doi:10.1111/j.1471-4159.2010.07132.x

12. Paul F. Pathology and MRI: exploring cognitive impairment in MS. *Acta Neurol Scand*. 2016;134(July):24-33. doi:10.1111/ane.12649

13. Stüber C, Morawski M, Schäfer A, et al. Myelin and iron concentration in the human brain: A quantitative study of MRI contrast. *Neuroimage*. 2014;93(P1):95-106.

doi:10.1016/j.neuroimage.2014.02.026

14. Varma G, Duhamel G, De Bazelaire C, Alsop DC. Magnetization transfer from inhomogeneously broadened lines: A potential marker for myelin. *Magn Reson Med*. 2015;73(2):614-622. doi:10.1002/mrm.25174

15. Girard OM, Prevost VH, Varma G, Cozzone PJ, Alsop DC, Duhamel G. Magnetization transfer from inhomogeneously broadened lines (ihMT): Experimental optimization of saturation parameters for human brain imaging at 1.5 Tesla. *Magn Reson Med*. 2015;73(6):2111-2121. doi:10.1002/mrm.25330

16. Varma G, Girard OM, Prevost VH, Grant AK, Duhamel G, Alsop DC. Interpretation of magnetization transfer from inhomogeneously broadened lines (ihMT) in tissues as a dipolar order effect within motion restricted molecules. *J Magn Reson*. 2015;260:67-76. doi:10.1016/j.jmr.2015.08.024

17. Duhamel G, Prevost VH, Cayre M, et al. Validating the sensitivity of inhomogeneous magnetization transfer (ihMT) MRI to myelin with fluorescence microscopy. *Neuroimage*. 2019;199(May):289-303. doi:10.1016/j.neuroimage.2019.05.061

18. Prevost VH, Girard OM, Mchinda S, Varma G, Alsop DC, Duhamel G. Optimization of inhomogeneous magnetization transfer (ihMT) MRI contrast for preclinical studies using dipolar relaxation time (T1D) filtering. *NMR Biomed*. 2017;30(6):1-13. doi:10.1002/nbm.3706

19. Mchinda S, Varma G, Prevost VH, et al. Whole brain inhomogeneous magnetization transfer (ihMT) imaging: Sensitivity enhancement within a steady-state gradient echo sequence. *Magn Reson Med*. 2018;79(5):2607-2619. doi:10.1002/mrm.26907

20. Van Obberghen E, Mchinda S, Le Troter A, et al. Evaluation of the sensitivity of inhomogeneous magnetization transfer (ihMT) MRI for multiple sclerosis. *Am J Neuroradiol*. 2018;39(4):634-641. doi:10.3174/ajnr.A5563

- 656 21. Munsch F, Varma G, Taso M, et al. Characterization of the cortical myeloarchitecture
657 with inhomogeneous Magnetization Transfer imaging (ihMT). *Neuroimage*.
658 2020;225(October 2020):117442. doi:10.1016/j.neuroimage.2020.117442
- 659 22. Geeraert BL, Lebel RM, Mah AC, et al. A comparison of inhomogeneous
660 magnetization transfer, myelin volume fraction, and diffusion tensor imaging measures
661 in healthy children. *Neuroimage*. 2018;182(May 2017):343-350.
662 doi:10.1016/j.neuroimage.2017.09.019
- 663 23. Ercan E, Varma G, Mädler B, et al. Microstructural correlates of 3D steady-state
664 inhomogeneous magnetization transfer (ihMT) in the human brain white matter
665 assessed by myelin water imaging and diffusion tensor imaging. *Magn Reson Med*.
666 2018;80(6):2402-2414. doi:10.1002/mrm.27211
- 667 24. Girard OM, Callot V, Prevost VH, et al. Magnetization transfer from inhomogeneously
668 broadened lines (ihMT): Improved imaging strategy for spinal cord applications. *Magn
669 Reson Med*. 2017;77(2):581-591. doi:10.1002/mrm.26134
- 670 25. Taso M, Girard OM, Duhamel G, et al. Tract-specific and age-related variations of the
671 spinal cord microstructure: A multi-parametric MRI study using diffusion tensor
672 imaging (DTI) and inhomogeneous magnetization transfer (ihMT). *NMR Biomed*.
673 2016;29(6):817-832. doi:10.1002/nbm.3530
- 674 26. Rasoanandrianina H, Demortière S, Trabelsi A, et al. Sensitivity of the Inhomogeneous
675 Magnetization Transfer Imaging Technique to Spinal Cord Damage in Multiple
676 Sclerosis. *AJNR Am J Neuroradiol*. 2020;41(5):929-937. doi:10.3174/ajnr.A6554
- 677 27. Rasoanandrianina H, Duhamel G, Feiweier T, et al. Regional and structural integrity of
678 the whole cervical spinal cord using 3D-T1 MP2RAGE and multi-slice multi angle
679 DTI and ihMT sequences at 3T : preliminary investigations on age-related changes .
680 In: *Proceedings 25th Scientific Meeting, International Society for Magnetic Resonance
681 in Medicine*. ; 2017;p.0912.
- 682 28. Association JO. Japanese Orthopaedic Association assessment criteria guidelines
683 manual. *Tokyo Japanese Orthop Assoc*. 1996:46-49.
- 684 29. Vernon H, Mior S. The neck disability index: A study of reliability and validity. *J
685 Manipulative Physiol Ther*. 1991;14(7):409-415.
- 686 30. Chung S, Kim D, Breton E, Axel L. Rapid B1+ mapping using a preconditioning RF
687 pulse with turboFLASH readout. *Magn Reson Med*. 2010;64(2):439-446.
688 doi:10.1017/S1355771817000310
- 689 31. Harris FJ. On the Use of Windows for Harmonic Analysis with the Discrete Fourier

Transform. *Proc IEEE*. 1978;66(1):51-83. doi:10.1109/PROC.1978.10837

32. Marques JP, Kober T, Krueger G, van der Zwaag W, Van de Moortele PF, Gruetter R. MP2RAGE, a self bias-field corrected sequence for improved segmentation and T1-mapping at high field. *Neuroimage*. 2010;49(2):1271-1281. doi:10.1016/j.neuroimage.2009.10.002
33. Kober T, Granziera C, Ribes D, et al. MP2RAGE multiple sclerosis magnetic resonance imaging at 3 T. *Invest Radiol*. 2012;47(6):346-352. doi:10.1097/RLI.0b013e31824600e9
34. Okubo G, Okada T, Yamamoto A, et al. MP2RAGE for deep gray matter measurement of the brain: A comparative study with MPRAGE. *J Magn Reson Imaging*. 2016;43(1):55-62. doi:10.1002/jmri.24960
35. Marques JP, Gruetter R. New Developments and Applications of the MP2RAGE Sequence - Focusing the Contrast and High Spatial Resolution R1 Mapping. *PLoS One*. 2013;8(7):e69294. doi:10.1371/journal.pone.0069294
36. Simioni S, Amarù F, Bonnier G, et al. MP2RAGE provides new clinically-compatible correlates of mild cognitive deficits in relapsing-remitting multiple sclerosis. *J Neurol*. 2014;261(8):1606-1613. doi:10.1007/s00415-014-7398-4
37. Massire A, Taso M, Besson P, Guye M, Ranjeva JP, Callot V. High-resolution multi-parametric quantitative magnetic resonance imaging of the human cervical spinal cord at 7T. *Neuroimage*. 2016;143:58-69. doi:10.1016/j.neuroimage.2016.08.055
38. Rasoanandrianina H, Massire A, Taso M, et al. Regional T1 mapping of the whole cervical spinal cord using an optimized MP2RAGE sequence. *NMR Biomed*. 2019;32(11):1-17. doi:10.1002/nbm.4142
39. Demortière S, Lehmann P, Pelletier J, Audoin B, Callot V. Improved cervical cord lesion detection with 3D-MP2RAGE sequence in patients with multiple sclerosis. *Am J Neuroradiol*. 2020;41(6):1131-1134. doi:10.3174/ajnr.A6567
40. Baucher G, Rasoanandrianina H, Levy S, et al. T1 mapping for microstructural assessment of the cervical spinal cord in the evaluation of patients with degenerative cervical myelopathy. *Am J Neuroradiol*. 2021;42(7):1348-1357. doi:10.3174/ajnr.A7157
41. Prevost VH, Girard OM, Varma G, Alsop DC, Duhamel G. Minimizing the effects of magnetization transfer asymmetry on inhomogeneous magnetization transfer (ihMT) at ultra-high magnetic field (11.75 T). *Magn Reson Mater Physics, Biol Med*. 2016;29(4):699-709. doi:10.1007/s10334-015-0523-2

42. Rangwala N, Varma G, Hackney D, Alsop DC. Quantification of myelin in the cervical spinal cord using inhomogeneous magnetization transfer imaging. In: *Proceedings 21st Scientific Meeting, International Society for Magnetic Resonance in Medicine.* ; 2013:p.350.
43. Troalen T, Callot V, Varma G, Guye M, Alsop DC, Girard OM. Cervical Spine inhomogeneous Magnetization Transfer (ihMT) Imaging Using ECG-Triggered 3D Rapid Acquisition Gradient-Echo (ihMT-RAGE). In: *Proceedings 27th Scientific Meeting, International Society for Magnetic Resonance in Medicine.* ; 2018:p.300.
44. Forodighasemabadi A, Troalen T, Soustelle L, Duhamel G, Girard O, Callot V. Towards minimal T1 and B1 contributions in cervical spinal cord inhomogeneous magnetization transfer imaging. In: *Proceedings 29th Scientific Meeting, International Society for Magnetic Resonance in Medicine.* ; 2020:p.1175.
45. Varma G, Munsch F, Girard OM, Duhamel G, Alsop DC. An inhomogeneous magnetization transfer (ihMT) quantification method robust to B1 and T1 variations in magnetization prepared acquisitions. In: *Proceedings 27th Scientific Meeting, International Society for Magnetic Resonance in Medicine.* ; 2019:p.4911.
46. De Leener B, Lévy S, Dupont SM, et al. SCT: Spinal Cord Toolbox, an open-source software for processing spinal cord MRI data. *Neuroimage.* 2017;145(October 2016):24-43. doi:10.1016/j.neuroimage.2016.10.009
47. Ashburner J, Friston KJ. Unified segmentation. *Neuroimage.* 2005;26(3):839-851. doi:10.1016/j.neuroimage.2005.02.018
48. Soustelle L, Lamy J, Le Troter A, et al. A Motion Correction Strategy for Multi-Contrast based 3D parametric imaging : Application to Inhomogeneous Magnetization Transfer (ihMT). *bioRxiv.* 2020. doi:10.1101/2020.09.11.292649
49. Helms G, Dathe H, Kallenberg K, Dechent P. High-resolution maps of magnetization transfer with inherent correction for RF inhomogeneity and T1 relaxation obtained from 3D FLASH MRI. *Magn Reson Med.* 2008;60(6):1396-1407. doi:10.1002/mrm.21732
50. Varma G, Girard OM, Mchinda S, et al. Low duty-cycle pulsed irradiation reduces magnetization transfer and increases the inhomogeneous magnetization transfer effect. *J Magn Reson.* 2018;296:60-71. doi:10.1016/j.jmr.2018.08.004
51. Fonov V, Evans A, McKinsty R, Almli C, Collins D. Unbiased nonlinear average age-appropriate brain templates from birth to adulthood. *Neuroimage.* 2009;47:S102. doi:10.1016/s1053-8119(09)70884-5

- 758 52. Fonov V, Evans AC, Botteron K, Almli CR, McKinsty RC, Collins DL. Unbiased
759 average age-appropriate atlases for pediatric studies. *Neuroimage*. 2011;54(1):313-
760 327. doi:10.1016/j.neuroimage.2010.07.033
- 761 53. De Leener B, Fonov VS, Collins DL, Callot V, Stikov N, Cohen-Adad J. PAM50:
762 Unbiased multimodal template of the brainstem and spinal cord aligned with the
763 ICBM152 space. *Neuroimage*. 2018;165(July 2017):170-179.
764 doi:10.1016/j.neuroimage.2017.10.041
- 765 54. Patenaude B, Smith SM, Kennedy DN, Jenkinson M. A Bayesian model of shape and
766 appearance for subcortical brain segmentation. *Neuroimage*. 2011;56(3):907-922.
767 doi:10.1016/j.neuroimage.2011.02.046
- 768 55. Winkler AM, Webster MA, Brooks JC, Tracey I, Smith SM, Nichols TE. Non-
769 parametric combination and related permutation tests for neuroimaging. *Hum Brain*
770 *Mapp*. 2016;37(4):1486-1511. doi:10.1002/hbm.23115
- 771 56. Winkler AM, Ridgway GR, Webster MA, Smith SM, Nichols TE. Permutation
772 inference for the general linear model. *Neuroimage*. 2014;92:381-397.
773 doi:10.1016/j.neuroimage.2014.01.060
- 774 57. Mori S, Oishi K, Jiang H, et al. Stereotaxic white matter atlas based on diffusion tensor
775 imaging in an ICBM template. *Neuroimage*. 2008;40(2):570-582.
776 doi:10.1016/j.neuroimage.2007.12.035
- 777 58. Hua K, Zhang J, Wakana S, et al. Tract probability maps in stereotaxic spaces:
778 Analyses of white matter anatomy and tract-specific quantification. *Neuroimage*.
779 2008;39(1):336-347. doi:10.1016/j.neuroimage.2007.07.053
- 780 59. Wakana S, Caprihan A, Panzenboeck MM, et al. Reproducibility of quantitative
781 tractography methods applied to cerebral white matter. *Neuroimage*. 2007;36(3):630-
782 644. doi:10.1016/j.neuroimage.2007.02.049
- 783 60. Castinel BH, Adam P, Milburn PD, et al. Epidemiology of cervical spine abnormalities
784 in asymptomatic adult professional rugby union players using static and dynamic MRI
785 protocols: 2002 to 2006. *Br J Sports Med*. 2010;44(3):194-199.
786 doi:10.1136/bjsm.2007.045815
- 787 61. Taki Y, Thyreau B, Kinomura S, et al. Correlations among brain gray matter volumes,
788 age, gender, and hemisphere in healthy individuals. *PLoS One*. 2011;6(7):e22734.
789 doi:10.1371/journal.pone.0022734
- 790 62. Jäncke L, Mérillat S, Liem F, Hänggi J. Brain size, sex, and the aging brain. *Hum*
791 *Brain Mapp*. 2015;36(1):150-169. doi:10.1002/hbm.22619

- 792 63. Rasoanandrianina H. Toward the characterization of macro and micro -traumatism of
793 the human cervical spinal cord in rugby. *PhD Thesis*. 2019.
- 794 64. Stamm JM, Koerte IK, Muehlmann M, et al. Age at First Exposure to Football Is
795 Associated with Altered Corpus Callosum White Matter Microstructure in Former
796 Professional Football Players. *J Neurotrauma*. 2015;32(22):1768-1776.
797 doi:10.1089/neu.2014.3822
- 798 65. Abbas K, Shenk TE, Poole VN, et al. Alteration of default mode network in high
799 school football athletes due to repetitive subconcussive mild traumatic brain injury: A
800 resting-state functional magnetic resonance imaging study. *Brain Connect*.
801 2015;5(2):91-101. doi:10.1089/brain.2014.0279
- 802 66. Koerte IK, Kaufmann D, Hartl E, et al. A prospective study of physician-observed
803 concussion during a varsity university hockey season: white matter integrity in ice
804 hockey players. Part 3 of 4. *Neurosurg Focus*. 2012;33(6):1-7.
- 805 67. Núñez MT, Urrutia P, Mena N, Aguirre P, Tapia V, Salazar J. Iron toxicity in
806 neurodegeneration. *BioMetals*. 2012;25(4):761-776. doi:10.1007/s10534-012-9523-0
- 807 68. Daglas M, Adlard PA. The Involvement of Iron in Traumatic Brain Injury and
808 Neurodegenerative Disease. *Front Neurosci*. 2018;12(December).
809 doi:10.3389/fnins.2018.00981
- 810 69. del C. Valdés Hernández M, Ritchie S, Glatz A, et al. Brain iron deposits and lifespan
811 cognitive ability. *Age (Omaha)*. 2015;37(5). doi:10.1007/s11357-015-9837-2
- 812 70. Hagemer J, Geurts JJG, Zivadinov R. Brain iron accumulation in aging and
813 neurodegenerative disorders. *Expert Rev Neurother*. 2012;12(12):1467-1480.
814 doi:10.1586/ern.12.128
- 815 71. Zhang J, Zhang Y, Wang J, et al. Characterizing iron deposition in Parkinson's disease
816 using susceptibility-weighted imaging: An in vivo MR study. *Brain Res*.
817 2010;1330:124-130. doi:10.1016/j.brainres.2010.03.036
- 818 72. Barbosa JHO, Santos AC, Tumas V, et al. Quantifying brain iron deposition in patients
819 with Parkinson's disease using quantitative susceptibility mapping, R2 and R2*. *Magn*
820 *Reson Imaging*. 2015;33(5):559-565. doi:10.1016/j.mri.2015.02.021
- 821 73. Bergsland N, Tavazzi E, Laganà MM, et al. White Matter Tract Injury is Associated
822 with Deep Gray Matter Iron Deposition in Multiple Sclerosis. *J Neuroimaging*.
823 2017;27(1):107-113. doi:10.1111/jon.12364
- 824 74. Oshiro S, Morioka MS, Kikuchi M. Dysregulation of iron metabolism in Alzheimer's
825 disease, Parkinson's disease, and amyotrophic lateral sclerosis. *Adv Pharmacol Sci*.

2011;2011. doi:10.1155/2011/378278

75. Kwan JY, Jeong SY, van Gelderen P, et al. Iron accumulation in deep cortical layers accounts for MRI signal abnormalities in ALS: Correlating 7 tesla MRI and pathology. *PLoS One*. 2012;7(4). doi:10.1371/journal.pone.0035241
76. Blecher R, Elliott MA, Yilmaz E, et al. Contact Sports as a Risk Factor for Amyotrophic Lateral Sclerosis: A Systematic Review. *Glob Spine J*. 2019;9(1):104-118. doi:10.1177/2192568218813916
77. Chiò A, Calvo A, Dossena M, Ghiglione P, Mutani R, Mora G. ALS in Italian professional soccer players: The risk is still present and could be soccer-specific. *Amyotroph Lateral Scler*. 2009;10(4):205-209. doi:10.1080/17482960902721634
78. Mark Haacke E, Reichenbach JR, Wang Y. Susceptibility-Weighted Imaging and Quantitative Susceptibility Mapping. *Brain Mapp An Encycl Ref*. 2015;1(1):161-172. doi:10.1016/B978-0-12-397025-1.00019-1
79. Loane DJ, Byrnes KR. Role of Microglia in Neurotrauma. *Neurotherapeutics*. 2010;7(4):366-377. doi:10.1016/j.nurt.2010.07.002
80. Hertanu A, Soustelle L, Le Troter A, et al. T 1D - weighted ihMT imaging – Part I. Isolation of long- and short- T 1D components by T 1D - filtering. *Magn Reson Med*. 2022;87(5):2313-2328. doi:10.1002/mrm.29139
81. King D, Hume PA, Brughelli M, Gissane C. Instrumented mouthguard acceleration analyses for head impacts in amateur rugby union players over a season of matches. *Am J Sports Med*. 2015;43(3):614-624. doi:10.1177/0363546514560876
82. King DA, Hume PA, Gissane C, Clark TN. Similar head impact acceleration measured using instrumented ear patches in a junior rugby union team during matches in comparison with other sports. *J Neurosurg Pediatr*. 2016;18(1):65-72. doi:10.3171/2015.12.PEDS15605
83. Langevin TL, Antonoff D, Renodin C, et al. Head impact exposures in women's collegiate rugby. *Phys Sportsmed*. 2021;49(1):68-73. doi:10.1080/00913847.2020.1770568